Enhanced Tunneling Electroresistance in Ferroelectric Tunnel Junctions due to the Reversible Metallization of the Barrier

Xiaohui Liu, J. D. Burton, and Evgeny Y. Tsymbal

Phys. Rev. Lett. **116**, 197602 — Published 11 May 2016

DOI: 10.1103/PhysRevLett.116.197602

Enhanced Tunneling Electroresistance in Ferroelectric Tunnel Junctions due to Reversible Metallization of Barrier

Xiaohui Liu, J. D. Burton* and Evgeny Y. Tsymbal†

Department of Physics and Astronomy & Nebraska Center for Materials and Nanoscience, University of Nebraska, Lincoln, Nebraska 68588-0299, USA

Realizing a large tunneling electroresistance (TER) effect is crucial for device application of ferroelectric tunnel junctions (FTJs). FTJs are typically composed of a thin ferroelectric layer sandwiched by two metallic electrodes, where TER generally results from the dependence of the effective tunneling barrier height on the ferroelectric polarization. Since the resistance depends exponentially not only on barrier height but also on barrier width, TER is expected to be greatly enhanced when one of the electrodes is a semiconductor where the depletion region near the interface can be controlled via ferroelectric polarization. To explore this possibility, we perform studies of $SrRuO_3/BaTiO_3/n$-$SrTiO_3$ FTJs, where n-$SrTiO_3$ is an electron doped $SrTiO_3$ electrode, using first-principles density functional theory (DFT). Our studies reveal that, in addition to modulation of the depletion region in n-$SrTiO_3$, the $BaTiO_3$ barrier layer becomes conducting near the interface for polarization pointing into n-$SrTiO_3$, leading to dramatic enhancement of TER. The effect is controlled by the band alignment between the semiconductor and the ferroelectric insulator and opens the way for experimental realization of enhanced TER in FTJs through the choice of a semiconducting electrode and interface engineering.

Studies of ferroelectric tunnel junctions (FTJs) have risen due to the promise of applications as electronic devices.[1,2,3] Usually a FTJ is composed of a few nanometer thick ferroelectric film sandwiched between two metal electrodes, where electronic transport is dominated by tunneling. The reversal of ferroelectric polarization in the barrier results in a change of resistance, leading to an electrically switchable on/off state, an effect known as tunneling electroresistance (TER). Metal-electrode based FTJs have already demonstrated off/on resistance ratios of a few hundred.[4, 5,6, 7] Further increasing the TER effect may assist in the prospect for FTJs in electronic device applications.

In a FTJ with two dissimilar metallic electrodes the reversal of ferroelectric polarization leads to a change in the effective tunneling barrier height because of the different screening length of the two metal electrodes [8,9]. In addition to barrier height, however, tunneling resistance is also exponentially dependent on barrier width. This opens the possibility of another mechanism to improve the TER.[8] The change of barrier width in a FTJ with two metal electrodes, however, is generally negligible due to the small screening length and large Fermi energy of metals. Conversely, an electrode with large screening length and small Fermi energy is required to accommodate changes in the effective tunnel barrier width by ferroelectric polarization reversal.

Due to their low carrier density, semiconductors have a much larger screening length and smaller Fermi energy compared to metals. With one electrode substituted by a semiconductor, i.e. in a metal(M)/ferroelectric(FE)/ semiconductor(SC) FTJ, reversal of ferroelectric polarization is expected to dramatically change the barrier profile and therefore the tunneling resistance. Recently, such a FTJ has been realized in experiment with a $Pt/BaTiO_3/Nb$:$SrTiO_3$ heterostructure.[10] $BaTiO_3$ is a prototypical ferroelectric, one electrode is a good metal, Pt, and the other is an n-type semiconductor, Nb:$SrTiO_3$. A large TER of ~10^4 was reported, which is a great improvement compared to FTJs having two metal electrodes. This experimental result is explained by depleting or accumulating carriers in an area near the interface between BTO/n-$SrTiO_3$ controlled by the ferroelectric polarization orientation. Specifically, when the ferroelectric polarization is pointing away from the semiconductor, a depletion region in Nb:$SrTiO_3$ near the interface results an additional barrier, increasing the effective tunnel barrier width compared to the case of opposite polarization orientation. From the view of electronic structure, this refers to the influence of ferroelectric polarization on the position of the conduction band minimum (CBM) with respect to the Fermi level.

In this paper, based on first-principles calculation and electrostatic modelling, we argue that this is just part of the picture for M/FE/SC FTJs. The whole picture should take into account not only the polarization charge screening by the semiconducting electrode, but also the band alignment between the electrode and the ferroelectric insulator. When the bands are aligned in such a way that the interfacial barrier (i.e. a potential step created by a ferroelectric insulator for tunneling electrons at the interface) is smaller than the polarization-induced potential drop, for polarization pointing into the semiconductor, the interfacial ferroelectric region becomes conducting which reduces the effective barrier width. This reversible interfacial metallization of ferroelectric in conjunction with the Schottky barrier formed in the semiconducting electrode for the opposite polarization orientation leads to a significant change in the barrier width with ferroelectric polarization switching, resulting in an enhanced TER.

First-principles calculations are performed using QuantumESPRESSO [11] within the local density approximation (LDA) and LDA+U. To model the M/FE/SC FTJ, we considered a heterostructure with 8 unit cells of ferroelectric $BaTiO_3$. One electrode is metallic $SrRuO_3$ and the other electrode is electron doped $SrTiO_3$. Both interfaces of this heterostructure are terminated with SrO/TiO_2. The doping concentration in *n*-$SrTiO_3$ is 0.09 electrons per formula unit (f.u.) realized by the virtual crystal approximation on the O sites. The supercell is constructed by stacking unit cells along the [001] direction (*z* direction). The in-plane lattice constant of the supercell is constrained to the calculated LDA lattice constant of cubic $SrTiO_3$, a = 3.871 Å, which corresponds to an in-plane strain of about -2.1% on $BaTiO_3$. This strain keeps the polar displacement normal to the interface.

Atomic relaxations are performed in the absence of U until forces are converged to less than 20 meV/Å. We find two stable states with opposite ferroelectric polarization in the $BaTiO_3$ layer. The polar displacements in each atomic layer are shown in Figure 1. We see that at the $BaTiO_3$/*n*-$SrTiO_3$ interface, polarization reversal induces a dramatic change in displacement profile. The continuation of polar displacements in *n*-$SrTiO_3$ near the interface from $BaTiO_3$ is a response to the electric field near the interface, penetrating about four unit cells (~ 2 nm).

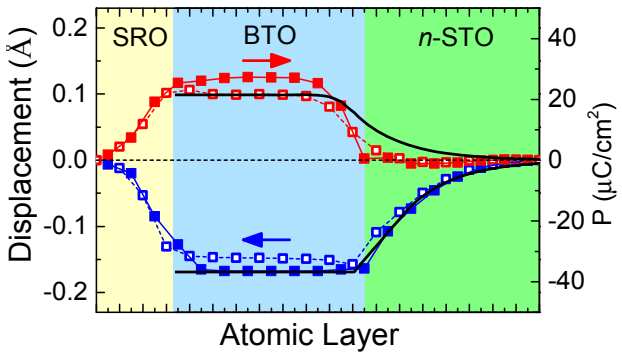

FIG. 1. Relative *z*-displacement between metal cation and anion (oxygen) in each atomic layer of the $SrRuO_3/BaTiO_3$/*n*-$SrTiO_3$ supercell. Filled symbols correspond to BO_2 layers (B = Ru or Ti) and open symbols correspond to AO layers (A = Sr or Ba). Red and blue curves correspond to polarization pointing into or away from the *n*-$SrTiO_3$ electrode, respectively. Black curves correspond to the polarization extracted from the electrostatic model described in the text.

To reveal the effect of polarization reversal on the electronic structure of the $BaTiO_3$/*n*-$SrTiO_3$ interface, we calculate the local density of states (LDOS) on the TiO_2 layers in each unit cell near the $BaTiO_3$/*n*-$SrTiO_3$ interface, as shown in Figure 2. In this calculation, U = 5 eV is applied to the Ti sites inside $BaTiO_3$ in order to correct for the reduced band-gap in the LDA.[12] The results for different U are presented in the Supplementary Information. The CBM profile can be extracted from the first-principles LDOS by tracking the energy of narrow semi-core states, e.g. Ti-3*s*, across the supercell.[13] Comparing the energy of these states relative to the position of the CBM determined from separate bulk calculations we can find the profile across the system, as shown by the points in Fig 2.

When polarization is pointing away from *n*-$SrTiO_3$, we find a slight band bending in *n*-$SrTiO_3$ near the interface, resulting in depletion of electrons by the negative polarization charge at the interface, as shown in Figure 2(b). The corresponding electric field gives rise to the polar displacements in the *n*-$SrTiO_3$, as shown in Fig. 1. These displacements correspond to the large lattice contribution to screening known for $SrTiO_3$ which dramatically increases the screening length and reduces the effect of screening by free carriers. This results in a muted bending of the CBM in *n*-$SrTiO_3$, and a narrow depletion region (~1 unit cell) being added to the effective tunnel barrier.

When polarization is pointing into *n*-$SrTiO_3$, however, the effective tunneling barrier width is dramatically reduced by the formation of a conducting layer in $BaTiO_3$ near the interface. As is shown in Figure 2(a), when polarization is pointing into *n*-$SrTiO_3$, the CBM of $BaTiO_3$ dips below the Fermi level for about 2 unit cells near the interface, corresponding to electrons being spilled into $BaTiO_3$ from the *n*-$SrTiO_3$ electrode. This is due to a relatively small interfacial barrier height (i.e. potential step at the $BaTiO_3$/*n*-$SrTiO_3$ interface) between the electron doped semiconductor and the ferroelectric.

We can estimate the barrier height between *n*-$SrTiO_3$ and $BaTiO_3$ by comparing the electron affinity of $SrTiO_3$ and $BaTiO_3$ bulk insulators. Previous studies have shown that the electron affinities of $BaTiO_3$ and $SrTiO_3$ are 3.9 and 4.0 eV, respectively, [14] which implies that the CBM minimum in $SrTiO_3$ lies about 0.1 eV below the CBM of $BaTiO_3$. This result is consistent with the photoemission studies of a $BaTiO_3/SrTiO_3$ heterojunction, showing a band offset between $BaTiO_3$ and $SrTiO_3$ of about 0.1 eV.[15] Electron doping populates the conduction band of $SrTiO_3$ and reduces the barrier height seen by transport electrons. With a doping level of 0.09 *e*/u.c. the Fermi level is about 0.2 eV above the CBM of *n*-$SrTiO_3$, which means that the CBM of bulk $BaTiO_3$ lies below the Fermi level of *n*-$SrTiO_3$ by about 0.1 eV.

When the polarization is pointing into *n*-$SrTiO_3$ and the polarization-induced potential drop is larger than the built-in barrier height, spillage of electrons from *n*-$SrTiO_3$ into $BaTiO_3$ occurs. This is reflected by the position of the CBM of $BaTiO_3$ near the interface being

below the Fermi level as shown in Figure 2(a). We find that the effective tunneling barrier width is therefore reduced by about 2 unit cells with polarization pointing into *n*-$SrTiO_3$. Recent experimental and theoretical studies have also found this kind of interfacial electronic reconstruction in ferroelectric oxides. [16, 17, 18]

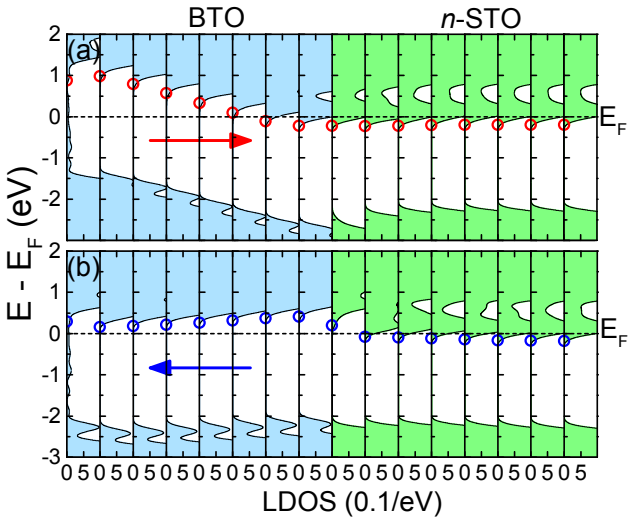

FIG. 2. Local density of states (LDOS) on the TiO_2 layers for ferroelectric polarization (a) into and (b) away from the $BaTiO_3$/*n*-$SrTiO_3$ interface. Circles indicate the position of the conduction band minimum, determined from the LDOS as described in the text.

The built-in electric field due to the work function step between *n*-$SrTiO_3$ and $SrRuO_3$ can also be discerned from Fig. 2. Recent studies on FTJs pointed out that the built-in electric field due to the work function step between two electrodes may affect the stability of ferroelectricity in the barrier. [19,20] This difference in work function leads to a relatively strong built-in electric field pointing from *n*-$SrTiO_3$ to $SrRuO_3$ across the $BaTiO_3$ barrier. When polarization is pointing into *n*-$SrTiO_3$, the depolarizing field is parallel to the built-in field and makes the band tilting in $BaTiO_3$ very strong, as can be seen from the CBM profile in Figure 2(a). When polarization is pointing away from *n*-$SrTiO_3$, however, the depolarizing field is antiparallel to the built-in field, leading to a relatively flat band profile in $BaTiO_3$, as shown in Figure 2(b), implying that the strength of the built-in electric field is comparable to the depolarizing field.

The effects of polarization on band alignment in such a FTJ can be demonstrated by a continuum electrostatic model, as described in the Supplemental Information. The effects of the metal $SrRuO_3$ electrode are incorporated by interfacial boundary conditions on the $BaTiO_3$ layer assuming a linearized Thomas-Fermi screening length λ, a relative dielectric constant ε and an intrinsic potential step ΔV_{SRO} across the interface. The effect of screening in $SrRuO_3$ only enters the boundary condition on $BaTiO_3$ as $\lambda/\varepsilon = 0.16$ Å, which we found in our previous work.[21] The polarization in $BaTiO_3$ is modeled in the linear response regime, $P(x) = P_0 + \chi_{BTO}\varepsilon_0 E(x)$, where $P_0 = 40$ μC/cm^2 is the calculated spontaneous polarization of bulk $BaTiO_3$ under compressive in-plane strain due to a $SrTiO_3$ substrate. χ_{BTO} is the linear dielectric susceptibility which accounts for deviations from the bulk polarization due to an electric field. Similarly, we define a linear susceptibility for $SrTiO_3$, χ_{STO}. The local electron densities in both $BaTiO_3$, $n_{BTO}(x)$, and *n*-$SrTiO_3$, $n_{STO}(x)$, are determined self-consistently with the potential by incorporating an averaged LDOS of the conduction band shifted by the local potential $-e\varphi(x)$ (see Supplementary Information).

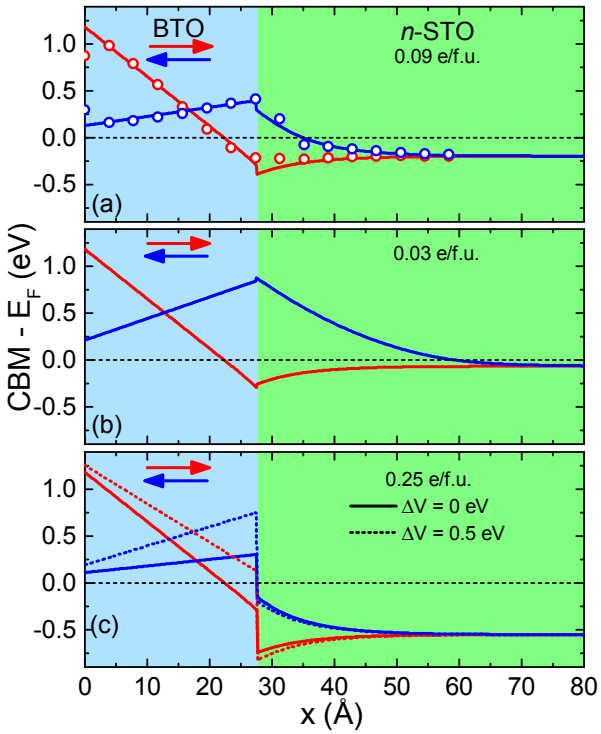

FIG. 3. Electrostatic model profile of the CMB in $BaTiO_3$ and *n*-$SrTiO_3$ for doping concentration (a) $n_0 = 0.09$ *e*/f.u. (b) 0.03 *e*/f.u. and (c) 0.25 *e*/f.u. Red and blue curves correspond to polarization pointing into and away-from *n*-$SrTiO_3$, respectively, with the parameters provided in the text. The points in (a) are the CBM extracted from the LDOS as described in the text. Dashed curves in (c) include an additional intrinsic potential step $\Delta V = 0.5$ eV across the $BaTiO_3$/*n*-$SrTiO_3$ interface.

The undefined quantities of the model described above are used as fitting parameters and the best fit to the CBM profile corresponds to $\Delta V_{SRO} = 0.89$ V, $\chi_{STO} = 78$ and $\chi_{BTO} = 39$. The resulting model CBM profile is

plotted as the solid curves in Fig. 3(a) for both polarization orientations, demonstrating a good agreement with the first-principles data. The corresponding model polarization profile is plotted along with the polar displacements in Fig. 1.

From Figure 3(a), we can see that this electrostatic model quantitatively match our first-principles calculations as shown in Figure 2. When polarization is pointing into n-$SrTiO_3$, the CBM of $BaTiO_3$ near the interface is below the Fermi energy as shown by the red curve, and a conducting layer forms near the interface in $BaTiO_3$. This conducting layer reduces the tunneling barrier width and contributes to the large TER effect in such a FTJ. The doping level n_0 = 0.09 e/f.u. is quite high compared to what might be used experiment due to computational limitations on the size of the supercell in first-principles calculations: a smaller doping concentration would lead to an intractably large screening length in n-$SrTiO_3$.[22] The electrostatic model does not suffer from this limitation. Keeping all other parameters fixed, in Fig. 3(b) we show the CBM profile for n_0 = 0.03 e/f.u. For this lower doping level, we see that the size of the depletion region in n-$SrTiO_3$ is considerably enhanced for polarization pointing away from the interface, indicating a dramatic increase in the barrier width. For polarization pointing into the interface, however, the reduced barrier width remains unaffected, i.e. a conducting region is still formed inside the $BaTiO_3$ layer.

Based on the above predicted modulation of the CBM profile, we expect this system to exhibit a large TER effect. To explore this we perform first-principles transmission calculations as implemented in QuantumESPRESSO[11] with the supercell as a central scattering region. This scattering region is connected to a half infinite $SrRuO_3$ electrode on the left and another half infinite n-$SrTiO_3$ on the right. Transmission coefficients are determined by matching of (pseudo)wavefunctions in the scattering region with states in the electrodes for each in-plane momentum, $\mathbf{k}_{\|}$. [23, 24]

Our calculations confirm that the tunnel junction indeed exhibits much higher tunneling resistance with polarization pointing into n-$SrTiO_3$. The transmission at the Fermi energy for each $\mathbf{k}_{\|}$ in the two-dimensional Brillouin zone (2DBZ) is shown in Figs. 4(c,d) for the two polarization states. The transmission distribution in the 2DBZ is determined by the overlap of the Fermi surface projections of bulk n-$SrTiO_3$ and $SrRuO_3$, which explains its similar shape for the two polarization states. As is seen from Figures 4 (a, b), this shape is largely formed from the Fermi surface of n-$SrTiO_3$. The total transmission is calculated as the integral over the 2DBZ. We find that for polarization pointing into or away from n-$SrTiO_3$ the resistance-area products are 4.39×10^5 Ωμm^2 and 1.00×10^9 Ωμm^2, respectively. This implies that the off/on resistance ratio is about 2.3×10^4. These results are obtained for U = 5 eV on the Ti sites in $BaTiO_3$, but other values of U produce qualitatively similar results, as shown in the Supplementary Information.

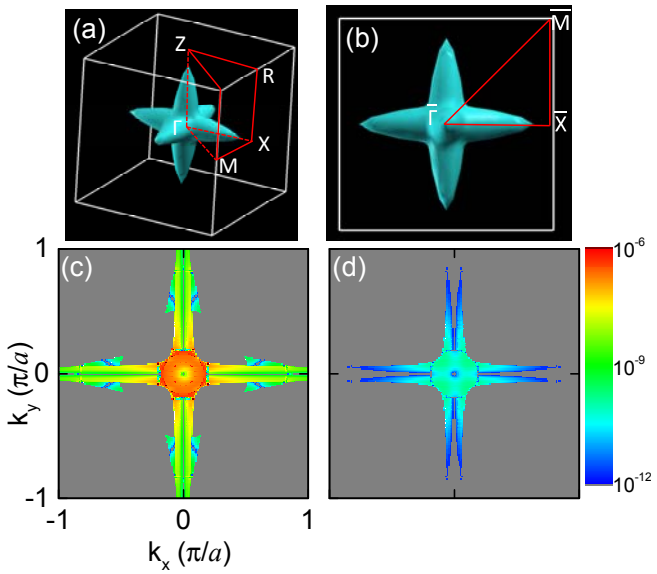

FIG. 4. (a) Fermi surface of n-$SrTiO_3$ and (b) its projection along the z-direction. (c, d) $\mathbf{k}_{\|}$-resolved transmission through the tunnel junction with polarization pointing into (c) and away (d) from n-$SrTiO_3$.

Our results have important implications for the design of FTJs with enhanced TER. Using a semiconducting electrode with a similar electron affinity to that of the ferroelectric insulator allows elimination of the Schottky barrier for one of the polarization states. This kind of FTJ provides a polar switch between a wide barrier formed jointly by a ferroelectric insulator and a depleted semiconductor, and a narrow barrier resulting from the metallized interface region within the ferroelectric. Furthermore, the proper matching between the bands at the interface may be obtained through interface engineering where the band alignment is controlled by the interface termination and the intrinsic interface dipole. [25,26,27]

As an example, the dashed curves in Fig. 3(c) display the results of a model calculation where we assumed the electron concentration of n_0 = 0.25 e/f.u. and included a potential step (i.e. a dipole layer) of ΔV = 0.5 eV at the $BaTiO_3$/n-$SrTiO_3$ interface. This situation can be viewed as representing a FTJ with a generic metallic oxide electrode rather than n-type $SrTiO_3$. Due to the high electron concentration and the interface potential step, there is no either polarization induced depletion region or metallization of the ferroelectric barrier. The TER effect arises in this case entirely due to the change in average

barrier height, with the right polarization state having higher resistance. Reducing or removing the dipole at this interface through interface engineering, however, leads to the TER of *opposite* sign, where the right polarization state has lower resistance due to metallization of the tunneling barrier (Fig. 3(c), solid lines).

We propose to explore this effect experimentally, using $La_{0.7}Sr_{0.3}MnO_3/BaTiO_3/La_{1-x}Sr_xO/La_{0.7}Sr_{0.3}MnO_3$ FTJs, where stoichiometry of the interfacial $La_{1-x}Sr_xO$ monolayer controls the Schottky barrier height. [25, 26] When x is reduced, the Fermi energy of $La_{0.7}Sr_{0.3}MnO_3$ approaches bottom of the $BaTiO_3$ conduction band, resulting in metallization of $BaTiO_3$ when its polarization points to the engineered interface. This is expected to reverse the TER sign, revealing a change in the mechanism controlling TER from barrier height modulation to barrier reversible metallization, which could be detected experimentally.

In summary, we have studied the effect of ferroelectric polarization on the TER effect in a M/FE/SC FTJ taking $SrRuO_3/BaTiO_3/n$-$SrTiO_3$ as a model system. Our study provides a comprehensive picture of the band alignment in a ferroelectric tunnel junction with a semiconducting electrode and helps to theoretically understand the huge TER effect of such a system. We find that, in addition to the polarization screening in n-$SrTiO_3$ leading to the depletion region near the interface for the OFF state, a metallic interface is formed reducing the barrier width in the ON state. The effect is controlled by the band alignment between the semiconductor and the ferroelectric insulator and opens the way for experimental realization of enhanced TER in FTJs through the choice of a semiconducting electrode and interface engineering. Thus, we hope our studies will aid in the design of future experiments and improve the functional prospects of FTJs.

This research was supported by the National Science Foundation (NSF) through Materials Research Science and Engineering Center (MRSEC, grant no. DMR-1420645) and by the Nanoelectronics Research Initiative through the Center for Nanoferroic Devices (CNFD). Computations were performed at the University of Nebraska Holland Computing Center.

* E-mail: jdburton1@gmail.com
† E-mail: tsymbal@unl.edu

[1] E. Y. Tsymbal and H. Kohlstedt, Science **313**, 181 (2006).
[2] E. Y. Tsymbal, A. Gruverman, V. Garcia, M. Bibes, and A. Barthélémy, MRS Bulletin **37**, 138 (2012).
[3] V. Garcia and M. Bibes, Nature. Comm. **5**, 4289 (2014).
[4] D. Pantel, S. Goetze, D. Hesse, and M. Alexe, *ACS Nano* **5**, 6032 (2011).
[5] A. Chanthbouala, A. Crassous, V. Garcia, K. Bouzehouane, S. Fusil, X. Moya, J. Allibe, B. Dlubak, J. Grollier, S. Xavier *et al.*, Nature Nano. **7**, 101 (2012).
[6] D. Pantel, H. D. Lu, S. Goetze, P. Werner, D. J. Kim, A. Gruverman, D. Hesse, and M. Alexe, Appl. Phys. Lett. **100**, 232902 (2012).
[7] G. Radaelli, D. Gutiérrez, F. Sánchez, R. Bertacco, M. Stengel, and J. Fontcuberta, Adv. Mater. **27**, 2602 (2015).
[8] M. Y. Zhuravlev, R. F. Sabirianov, S. S. Jaswal, and E. Y. Tsymbal, Phys. Rev. Lett. **94**, 246802 (2005).
[9] A. Gruverman, D. Wu, H. Lu, Y. Wang, H. W. Jang, C. M. Folkman, M. Y. Zhuravlev, D. Felker, M. Rzchowski, C. B. Eom, and E. Y. Tsymbal, Nano Lett. **9**, 3539 (2009).
[10] Z. Wen, C. Li, D. Wu, A. Li, and N. Ming, Nature Mater. **12**, 617 (2013).
[11] P. Giannozzi *et al.*, J. Phys.: Cond. Mat. **21**, 395502 (2009).
[12] In the absence of U the CBM resides slightly below the Fermi level across the $BaTiO_3$ barrier for polarization to the left, as shown in the Supplementary Information. This tiny occupation has very little effect on the atomic relaxation, but opens a spurious channel for transmission. Putting U on the Ti in $BaTiO_3$ corrects for this, but does not remove the metallization at the $BaTiO_3/n$-$SrTiO_3$ interface, indicating that this is a genuine physical characteristic of this interface.
[13] K. Janicka, J. P. Velev, and E. Y. Tsymbal, Phys. Rev. Lett. **102**, 106803 (2009).
[14] T. J. Zhang, R. K. Pan, Z. J. Ma, M. G. Duan, D. F. Wang, and M. He, Appl. Phys. Lett. **99**, 182106 (2011).
[15] S. Balaz, Z. Zeng, and L. J. Brillson. J. Appl. Phys. **114**, 183701 (2013)
[16] M. S. J. Marshall, A. Malashevich, A. S. Disa, M.-G. Han, H. Chen, Y. Zhu, S. Ismail-Beigi, F. J. Walker, and C. H. Ahn, Phys. Rev. Appl. **2**, 051001 (2014).
[17] K. D. Fredrickson and A. A. Demkov, Phys. Rev. B **91**, 115126 (2015).
[18] A. Quindeau, V. Borisov, I. Fina, S. Ostanin, E. Pippel, I. Mertig, D. Hesse, and M. Alexe, Phys. Rev. B **92**, 035130 (2015).
[19] S. Boyn, V. Garcia, S. Fusil, C. Carrétéro, K. Garcia, S. Xavier, S. Collin, C. Deranlot, M. Bibes, and A. Barthélémy, APL Materials **3**, 061101 (2015).
[20] Y. Liu, X. Lou, M. Bibes, and B. Dkhil, Phys. Rev. B **88**, 024106 (2013).
[21] X. Liu, Y. Wang, J. D. Burton, and E. Y. Tsymbal, Phys. Rev. B **88**, 165139 (2013).
[22] J. M. Ziman, *Principles of the Theory of Solids* (Cambridge University Press, Cambridge, UK, 1964).
[23] H. J. Choi and J. Ihm, Phys. Rev. B **59**, 2267 (1999).
[24] A. Smogunov, A. Dal Corso, and E. Tosatti, Phys. Rev. B **70**, 045417 (2004).
[25] Y. Hikita, M. Nishikawa, T. Yajima, and H. Y. Hwang, Phys. Rev. B **79**, 073101 (2009).
[26] J. D. Burton, and E. Y. Tsymbal, Phys. Rev. B **82**, 161407R (2010).
[27] H. Lu *et al.*, Adv. Mater. **24**, 1209 (2012).